A Relaxation Oscillator Description of the Burst-Generating Mechanism in the Cardiac Ganglion of the Lobster, *Homarus americanus*

EARL MAYERI

From the Department of Zoology and Bodega Marine Laboratory, University of California, Berkeley, California 94720. Dr. Mayeri's present address is the Department of Physiology, University of California, San Francisco, California 94143.

ABSTRACT Properties of the neural mechanism responsible for generating the periodic burst of spike potentials in the nine ganglion neurons were investigated by applying brief, single shocks to the four small cells with extracellular electrodes placed near the trigger zones of the small cells. The shock elicited a burst if presented during the latter portion of the silent period, terminated a burst during the latter portion of the burst period, and was followed by a newly initiated burst during the early portion of the burst period. The resultant changes in burst and silent period durations were quantitatively described by a second-order non-linear differential equation similar to the van der Pol equation for a relaxation oscillator. The equation also qualitatively described changes in firing threshold of the small cells during the burst cycle. The first derivative of the solution to the equation is similar to slow transmembrane potentials in neurons that are involved in generation of burst activity in other crustacean cardiac ganglia.

INTRODUCTION

Burst activity is a feature common to many neural subsystems that control behavior. In arthropods it is involved in the control of heartbeat, gastric mill, locomotion, insect flight, swimmeret movement, and cricket song, among others (for reviews, see Wilson 1970; Evoy and Cohen, 1972). Though these neural subsystems have been the subject of intensive study, the mechanisms responsible for the genesis of burst activity remain to be convincingly demonstrated (Wilson, 1970). One reason for this is that not enough is known about the properties of burst-generating mechanisms, be it in populations of nerve cells (Wilson, 1966; Lewis, 1968), or in single burst-generating neurons (Strumwasser, 1967).

The anatomy and physiology of the cardiac ganglion of the Maine lobster, *Homarus americanus* is favorable for studying burst generator properties using extracellular recording and stimulating techniques. The ganglion neurons will discharge in an essentially normal manner for hours after isolation from the heart muscle. Brief single shocks delivered through stimulating electrodes placed at appropriate locations on the main trunk of the ganglion produce systematic changes in burst activity that are easily quantifiable. Spikes from individual neurons can be identified by recording simultaneously from four or more extracellular electrodes placed on the main trunk and principal nerves (Hartline, 1967 *b*; Mayeri, 1973).

The electrophysiology of *Homarus* and *Panulirus* cardiac ganglia has been studied in considerable detail (Hagiwara, 1961, and Mayeri, 1973). The results of the previous paper (Mayeri, 1973) suggest that the ganglion is functionally organized into two layers; one or more of the four small cells serve to generate the burst rhythm that is characteristic of this ganglion, and the small cells impose the burst rhythm on the five large cells via excitatory synaptic connections. The large cells are the motorneurons of the system. In the present account the properties of the burst-generating mechanism are examined in greater detail by exciting the small cells with brief, single shocks at different times in the burst cycle. The resultant modulations of burst activity, their dependence on stimulus strength, and major aspects of normal burst activity are described by a second order nonlinear differential equation for a relaxation oscillator that is similar in form to the van der Pol equation. The results reinforce the view that one or more small cells are individually capable of generating burst activity.

METHODS

Experiments were made on 67 specimens of *Homarus americanus* (600 g) using the techniques described in a previous paper (Mayeri, 1973). Recordings were made from eight Ag-$AgCl_2$ suction electrodes placed on the main trunk and principal nerves of the cardiac ganglion at locations that were appropriate for spike identification. Spike activity from any four of the electrodes was recorded on a tape recorder for later data analysis. Any two of the electrodes could also be used for electrical stimulation.

RESULTS

As described in the previous paper (Mayeri, 1973), brief, single shocks applied through two Ag-$AgCl_2$ suction electrodes to small cells can modulate burst according to the phase of the burst cycle at which the shock is presented. In the data presented here the electrodes were similarly placed about 1 mm apart on the main trunk of the ganglion near or slightly anterior to the origin of the postero-lateral nerves near the small cell trigger zones. Each shock was triggered at a fixed delay beyond the first small cell spike that initiates each burst. A shock of sufficient strength elicited a burst when presented during

the silent period, terminated a burst when presented during the latter portion of the burst period, and was followed by a "reset" burst, i.e. one of approximately normal duration, when presented during the early portion of the burst. Though stimulus threshold for these effects varied according to phase of the burst cycle (see below), only one strength was used, and it was chosen so as to produce all three types of burst modulation in the same preparation.

Elicited Bursts

The duration of an elicited burst was a function of the silent period from the end of the previous burst to the delivery of the shock, rather than some continuous function of stimulus strength. Elicited burst duration for a *particular* silent period was obtained by averaging the elicited burst durations of 25 separate trials. Also averaged in this manner were durations of the silent period and the spontaneous burst after the elicited burst.

Duration of the elicited burst as a function of the silent period from the end of the previous burst to the delivery of the shock is shown in Fig. 1 (circles). The earlier in the silent period the shock was delivered, the shorter was the elicited burst. In each case the silent period after the elicited burst was almost normal (4% longer) and so was the next burst duration. Sometimes the small cell initiating the elicited burst was not the same as the one initiating natural bursts, but the results in either case were qualitatively the same.

Terminated Bursts

When the shock was presented at any time during the last two-thirds of a natural burst, the shock terminated the burst immediately. Duration of the next silent period was less than normal, but the next burst duration was normal. Fig. 2 (another preparation) shows duration of the silent period immediately after the shock as a function of terminated burst duration (dots): the shorter the terminated burst, the shorter the following silent period. Silent periods after the terminated bursts were averaged for 25 trials in the manner described for the elicited bursts.

The primary difference between elicited and terminated bursts was the manner in which the shock constrained burst activity; the duration of the elicited burst depended on the magnitude of the silent period *preceding* the shock, whereas the duration of the terminated burst determined the magnitude of the silent period which *followed* the shock. Each case involved a relationship between burst duration and silent period, shown in Fig. 2, but the two relationships were not identical. For example, for the same magnitude of silent period (1380 ms) duration of the elicited burst was about normal, but duration of the terminated burst was 50% shorter than normal. Also, with elicited bursts the stimulating electrodes could be located anywhere on

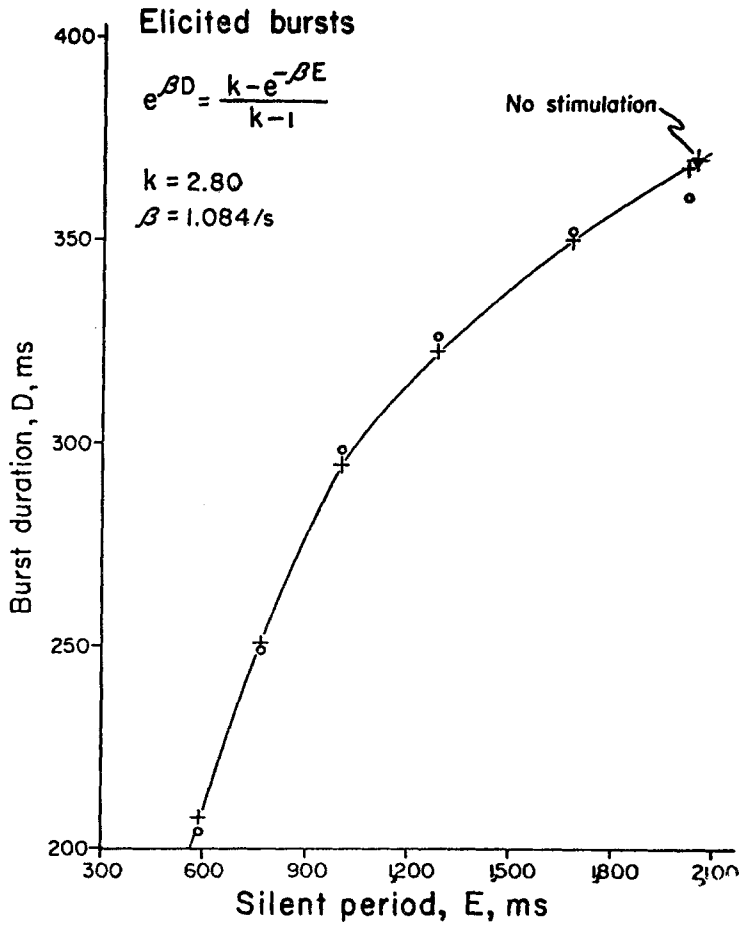

FIGURE 1. Duration of elicited bursts as a function of the silent period from the end of the previous burst to the first small cell spike of the elicited burst. Each circle is the average of 25 burst durations elicited for a particular silent period. The crosses are the best fit of the oscillator function to the experimental values (see text). The triangular point is average burst and silent period duration before stimulation began.

small cell axons, but with terminated bursts and reset bursts the electrodes had to be located near the small cell trigger zones.

"Reset" Bursts

When the shock was presented one-third of the way through a normal burst, the burst was not interrupted and its duration was normal. The shock, therefore, had little or no effect. However, a shock presented during the first third of the burst was followed by a burst which was usually of normal duration. In this case the shock seemed to terminate the ongoing burst and reset the

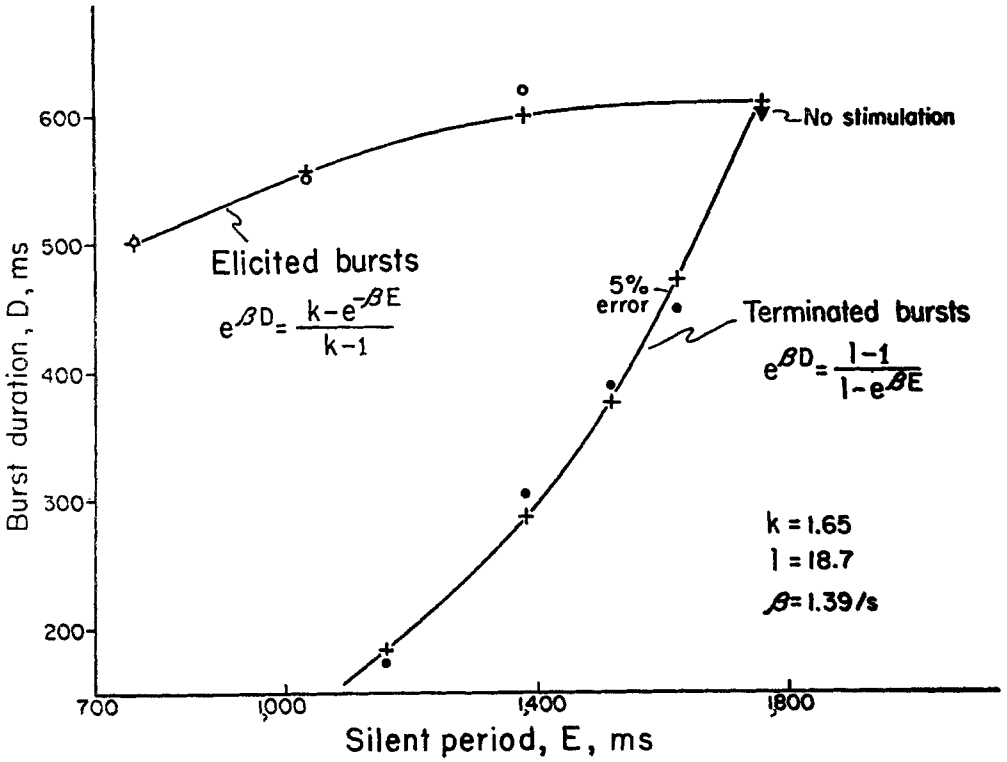

FIGURE 2. Average duration of elicited and terminated bursts. Durations of elicited bursts (circles) are plotted as in Fig. 1. Duration of the terminated burst (dots, ordinate values) determines the average duration of the silent period which follows it (abscissa values). Average natural burst and silent period durations (triangular point) were taken after stimulation for terminated bursts and before stimulation for elicited bursts. The crosses are the best fit of the oscillator function to the experimental values.

bursting mechanism to the start of a normal burst cycle because the burst immediately following the shock was normal as was the next silent period.

Oscillator Function Describing Modulation of Burst Activity

More intuitive insight for the systematic relationship between burst and silent period duration for both elicited and terminated bursts was gained by devising an oscillator function which describes the burst modulation results quite well. A nonlinear differential equation which has the oscillator function as its solution is derived in a later section.

The oscillator function $H(t)$ is shown in Fig. 3 (heaviest line) for one unstimulated cycle of burst and silent period. A burst is initiated when it reaches the threshold for burst initiation, S_{on}, at t_o. It increases exponentially during the burst until it reaches a second threshold S_{off}, at t_1 when the burst is ter-

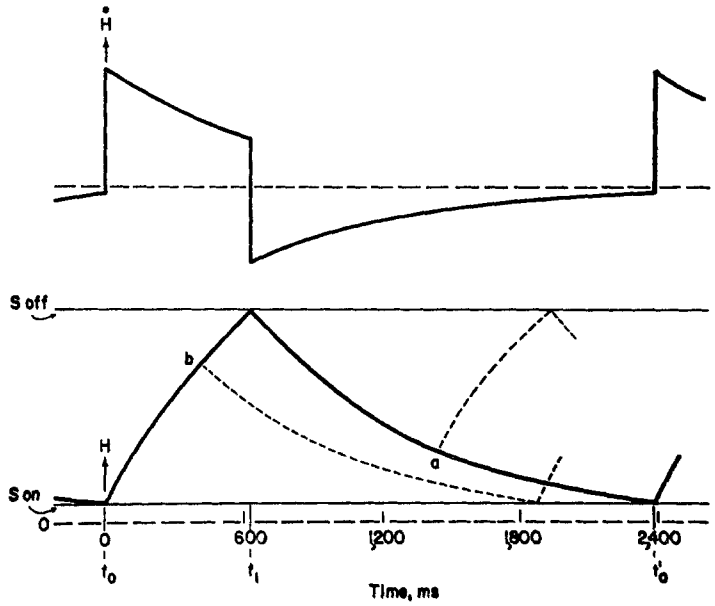

FIGURE 3. One cycle of the oscillator function, $H(t)$, and its first derivative, $\dot{H}(t)$, drawn according to parameters determined from the data of Fig. 2.

minated. During the silent period it decreases exponentially toward the asymptote at $H = 0$ until it reaches the threshold for burst initiation again.

During the burst period $H(t) = H_D(t)$, where

$$H_D(t) = A[1-e^{-\beta(t-t_0)}] + S_{on}e^{-\beta(t-t_0)}, \tag{1}$$

for $t_o \leq t \leq t_1$. A, S_{on}, S_{off}, and β are positive constants. During the silent period $H(t) = H_E(t)$, where

$$H_E(t) = S_{off}e^{-\beta(t-t_1)}, \tag{2}$$

for $t_1 \leq t \leq t_o'$.

The decay constant for the exponentials in Eqs. 1 and 2 are the same, but the coefficients and asymptotes for the two equations differ. This particular form was chosen because it seemed to be the simplest function in quantitative agreement with the data. The first derivative of the oscillator function with respect to time (Fig. 3) is similar to the membrane potential recorded intracellularly during burst activity in the cardiac ganglia of other crustaceans, but with spike potentials and membrane capacitance lacking (see Discussion).

ELICITED BURSTS If a burst is elicited during the silent period, the oscillator function starts to increase from its value at the instant the shock is applied (dashed line starting at *a*, Fig. 3), continuing until S_{off} is reached.

Burst duration for elicited bursts is less than normal because the oscillator function starts to increase from a value that is greater than for normal burst initiation. The silent period duration following the elicited burst is unaffected. Experimentally, single shock effects lasting beyond the burst immediately after the shock were small (see above), and they will therefore be ignored. By applying the boundary condition $H_D(t) = H_B(t)$ at the instant the shock is applied, the following expression is derived relating elicited burst duration, D, to the silent period, E, preceding it:

$$e^{\beta D} = \frac{k - e^{-\beta E}}{k - 1}, \tag{3}$$

where $k = A/S_{\text{off}}$.

A computer program was employed to find the best least squares fit of the equation to data points for the elicited bursts. By choosing appropriate values for the constants k and β, the least square error was found for predicted values of burst duration. The predicted values are shown as +'s in Fig. 1. Maximum error in the predicted values was just under 3%. This was the best fit of the data of four preparations attempted.

TERMINATED BURSTS If a shock terminates a burst, the oscillator function during the ensuing silent period decreases exponentially towards $H = 0$ from its value at the time the shock was applied (dashed line starting at b, Fig. 3). The duration of the silent period following terminated bursts is less than normal because the oscillator function starts to decrease from a value that is less than for normal burst termination. The equation relating duration of the terminated burst, D, to the subsequent silent period duration, E, is derived from Eqs. 1 and 2. It is

$$e^{\beta D} = \frac{(l - 1)}{l - e^{\beta E}}, \tag{4}$$

where $l = A/S_{\text{on}}$.

In Fig. 2 data for both elicited and terminated bursts from a single preparation were used to fit Eqs. 3 and 4, respectively. Additionally, the data point for spontaneous bursting, taken before stimulation began, was fitted to the equation

$$e^{\beta D} = \frac{(l - 1)\, e^{-\beta E}}{k - 1},$$

derived from Eqs. 1 and 2. The best predicted burst duration values are shown as +'s in Fig. 2. The oscillator function in Fig. 3 was drawn according to parameters obtained from these data.

Decrease in Small Cell Firing Threshold during the Silent Period

Only one stimulus strength was used to produce the modulations of burst activity shown in Figs. 1 and 2. In each case it was chosen so that bursts would be elicited early in the silent period and yet still be effective in terminating or resetting the burst when presented during the burst period. If the function $H(t)$ has a physical counterpart, one might expect the firing threshold for the small cells to decrease exponentially to some minimal value during the silent period, just as the difference between $H(t)$ and the threshold for burst initiation, S_{on}, is greatest at the start of the silent period and decreases exponentially during the silent period (Fig. 3). As shown in Fig. 4 this is indeed the case. The stimulus electrodes were placed 1 mm apart on the main trunk just anterior to the postero-lateral nerves. For the first 200 ms after the end of a burst it was not possible to excite a small cell at inten-

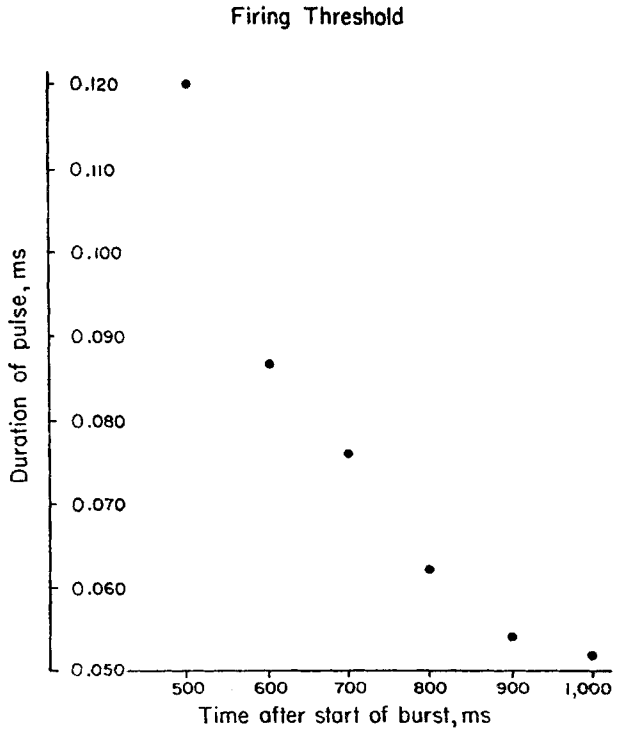

FIGURE 4. Decrease in small cell firing threshold during the silent period. The graph shows the duration of a shock just strong enough to excite a small cell spike as a function of the time interval from the start of a burst to the delivery of the shock. Durations of natural bursts and silent periods were 250 and 1150 ms, respectively. Stimulus voltage was 3.5 V. Stimulus electrodes were located on the main trunk near the small cell trigger zones.

sities which saturated the amplifiers of the recording electrodes. For shocks delivered later in the silent period the firing threshold decreased exponentially towards an asymptotic value. The time constant of the exponential was 511 ms. The large cells, on the other hand, showed little change of threshold throughout the burst cycle; the firing threshold for a typical large cell decreased 2 % in the first 200 ms. of the silent period and then was constant for the remainder of the silent period. This was another indication that the large cells are physiologically quite different from the small cells.

The time constant for firing threshold change of the small cells during the silent period was similar to the time constants, $1/\beta$, found by fitting the oscillator function to the data of Figs. 1 and 2, provided that allowances are made for differences in silent period duration by taking the ratio of normal silent period duration to the time constant in each case and comparing the ratios. The ratio for firing threshold data is 2.25, compared to 2.20 for the data of Fig. 1, and 2.45 for Fig. 2. The model is therefore consistent with changes in the firing threshold for small cells during the silent period.

Relaxation Oscillator Description of the Burst-Generating Mechanism

While it has been shown that the burst and silent period durations resulting from small cell stimulation are described by the oscillator function, an explanation of the changes in firing threshold throughout the burst cycle requires additional ad hoc assumptions. However, a differential equation for a relaxation oscillator was found to have a solution that is essentially the same as the oscillator function with the additional advantage of having threshold properties with striking similarities to those already described. The equation is: $\ddot{H} + F(\dot{H}) + H = 0$. $(\cdot)$ denotes differentiation with respect to time.

$$F(\dot{H}) \equiv \begin{cases} \frac{1}{\beta}\dot{H} - A, \text{for } \dot{H} > \beta(A - S_{\text{off}}) & \text{(burst period)} \\ -\frac{1}{\beta}\left(\frac{S_{\text{off}} - S_{\text{on}}}{A - S_{\text{off}} + S_{\text{on}}}\right)\dot{H} - \left(\frac{AS_{\text{on}}}{A - S_{\text{off}} + S_{\text{on}}}\right), & \\ \text{for } -\beta S_{\text{on}} \leq \dot{H} \leq \beta(A - S_{\text{off}}) & \text{(transition)} \\ \frac{1}{\beta}\dot{H}, \text{for } \dot{H} < -\beta S_{\text{on}}. & \text{(silent period)} \end{cases}$$

A, S_{off}, S_{on}, and β are the positive constants described previously; $A > S_{\text{off}} > S_{\text{on}}$. The equation is closely related to the van der Pol equation for a relaxation oscillator (see Stoker, 1950).

LIMIT CYCLE The piece-wise linear function $H = -F(\dot{H})$ is indicated in the phase-plane plot of Fig. 5. The figure has been drawn according to the parameter values obtained from the data of Fig. 2. The solution to the differential equation is a self-sustained oscillation denoted by the limit cycle. It

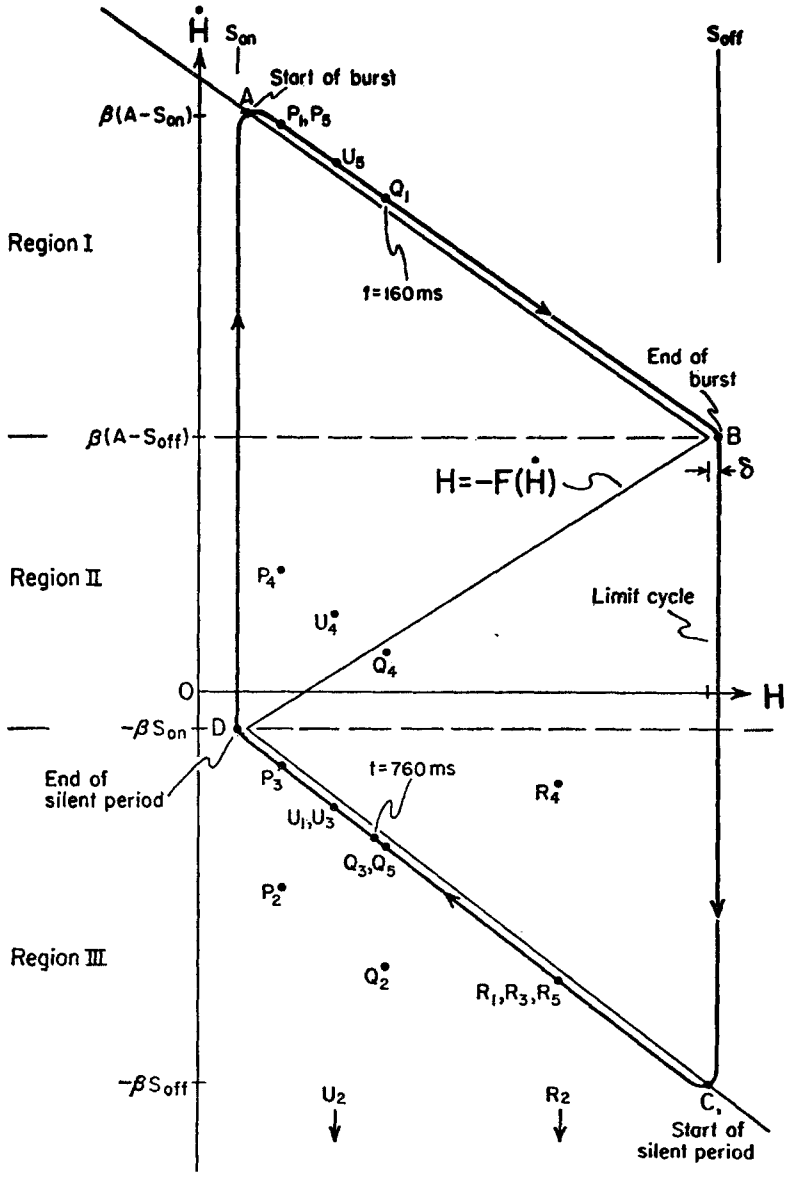

FIGURE 5. Phase-plane representation of the relaxation oscillator differential equation. Drawn according to the parameters determined from the data of Fig. 2.

was found by assuming initial conditions that were close to the limit cycle in one of the three regions of the phase plane (corresponding to the three domains of $\dot{H}$ over which $F(\dot{H})$ is defined), finding the solution of the second-order linear differential equation in the region, finding the point at which the trajectory intersects the boundary of the region, and using that point as

initial conditions for the solution in the next region. For a solution starting at A (Fig. 5) corresponding to the start of the burst, the limit cycle lies just beyond the line $H = -F(\dot{H})$ of region I. At B, the end of the burst period, the distance between the limit cycle and $H = -F(\dot{H})$ is approximately β^2 or 10^{-6} per ms^2 (Stoker, 1950). This means that the equations for the burst period and the silent period, given by the oscillator function (Eq. 1 and 2) are good approximations to the limit cycle of the relaxation oscillator in regions I and III, respectively.

During the transitional parts of the limit cycle from burst period to start of silent period, B–C, and from silent period to start of burst period, D–A, $|\dot{H}|$ changes very rapidly and $|H|$ is almost constant. In each case the time for the transition is about 0.01 ms.

SIMULATION OF SMALL CELL STIMULATION RESULTS Stimulation parameters for the relaxation oscillator were chosen to be of the simplest form and magnitude and yet mimic as many of the small cell stimulation results as possible. It was assumed that the effect of the stimulation on H was close to zero compared to the effect on $\dot{H}$, and that the change of $\dot{H}$ due to the stimulus was of the same magnitude, irrespective of the time during the burst cycle at which it was applied. An example of the stimulus is shown in Fig. 6. The stimulus lasts 0.8 ms, changing H hardly at all ($\Delta S \simeq 0$) and changing $\dot{H}$ first by an amount $\Delta \dot{S}_1$ (<0), and then by $\Delta \dot{S}_2$ (>0). $|\Delta \dot{S}_1| > |\Delta \dot{S}_2|$. A possible physical interpretation of this stimulus configuration is that $\Delta \dot{S}(t)$ is a simplified description of the stimulus current passing through the nerve cell membrane. The rectangular-wave stimulus is differentiated with respect to time by the capacitance of the ganglionic sheath which is in series with the stimulating electrodes.

In Fig. 5 the effect of the stimulus when applied within the first 150 ms of the burst is shown starting at point P_1. $\Delta \dot{S}_1$ displaces the system to P_2 but within .003 ms the system returns to P_3 on the limit cycle. $\Delta \dot{S}_2$ comes 0.8

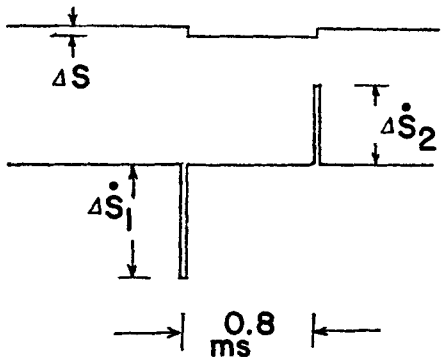

FIGURE 6. Stimulus used as a forcing function for the relaxation oscillator equation.

ms after $\Delta \dot{S}_1$, displacing the system from P_3 to P_4. P_4 is a highly unstable point as are all points outside the limit cycle, so the system returns to P_5 ($\simeq P_1$) within 0.007 ms. The overall effect of the stimulus is to return the system to its original state within 0.8 ms. This aspect of the model does not correspond to the experimental results, where stimulation in the first 150 ms of the burst period resulted in reset bursts. But it can be made to do so by assuming a more intricate stimulus wherein ΔS is larger, or membrane capacitative effects are included, while still retaining the other features of the stimulus presently employed.

The same shock applied at Q_1, 160 ms after the start of the burst, gives the proper results. $\Delta \dot{S}_1$ takes the system to Q_2, and it returns quickly to Q_3. However, $\Delta \dot{S}_2$ is not strong enough to drive the system above the line DB, and the system returns from Q_4 to a point on the silent period portion of the limit cycle, Q_5. Thus, as found experimentally, the effect of stimulation at this point and for later points in the burst period is to terminate the bursts, and the relationship between terminated burst duration and ensuing silent period duration given by Eq. 4 is shown as the solid line for terminated bursts in Fig. 2.

For elicited bursts, a shock delivered early in the silent period at R_1 (Fig. 5) is not sufficient to reach threshold for initiation of a burst (R_4 is below the line DB). But a shock delivered later than 760 ms into the silent period, at U_1, is sufficient to elicit a burst, as was found experimentally. The relationship between elicited burst duration and duration of the preceding silent period, given by Eq. 3 and described by the solid line for elicited bursts in Fig. 2 is also similar to experimental values.

THRESHOLD CHANGES Changes in firing threshold during the silent period are consistent with the relaxation oscillator description. The firing threshold is determined by the magnitude of the difference between the characteristic, $F(\dot{H})$, in regions II and III (lines BD and CD in Fig. 6). Denoting the difference by ΔT_h, it is given by

$$\Delta T_h = (\beta A)\,(H_E - S_{on})/(S_{off} - S_{on}),$$

and since $H_E = S_{off}\, e^{-\beta(t-t_1)}$, the decay constant for the firing threshold during the silent period is the same as the one associated with changes in elicited burst duration.

There is qualitative evidence to suggest that during the burst period the firing threshold for the small cells increased in a manner that is also consistent with the relaxation oscillator description. For the small cell stimulation data of Fig. 2 only one stimulus intensity was used. Over a certain region of the burst cycle, one that extended from the latter portion of the silent period through approximately the first third of the burst period, the shock was strong

enough to be followed immediately by another burst. The limits of this region were from 760 ms after the silent period began, to 140 ms after the start of the next burst period. The value of the oscillator function $H(t)$ at the two limits of the region is the same, 0.36 times the value of S_{off} (Fig. 5). Within the region, $H(t)$ is less than at the limits of the region, and the shock is strong enough to be followed immediately by another burst. For parts of the burst cycle outside of the region, $H(t)$ is greater than the value at the limits, and the shock is below the intensity necessary to elicit another burst.

Also, if the shock intensity was increased above its original value, the shock was effective in initiating bursts later in the burst period and earlier in the silent period. These changes are also to be expected of the relaxation oscillator. For instance, in Fig. 5 if the shock delivered at 160 ms in the burst period (Q_1–Q_6) is increased, then the point Q_4 will be above the line DB and the stronger shock will be followed by a burst. Near the end of the natural burst no burst could be initiated at the strongest intensities employed. For shocks presented during the burst period at or before 140 ms with an intensity lower than the original, the burst could sometimes be terminated without being reset. The relaxation oscillator also simulates these results.

Thus the relaxation oscillator quantitatively describes the results of Fig. 2 and is qualitatively consistent with the firing threshold properties of the small cells throughout the burst cycle.

DISCUSSION

The results of the accompanying paper (Mayeri, 1973) suggest that one or more small cells generate the burst discharge in the lobster cardiac ganglion, and that these cells impose the burst pattern on the remaining cells by excitatory synaptic drive. Two classes of burst-generating mechanisms have been suggested for the cells which are responsible for burst production. One of them assumes that each cell is inherently capable of discharging spontaneously at constant low frequency when functionally isolated from the others. Bursts are formed because of mutual synaptic excitation among them. A burst is initiated by a single spontaneous spike in one small cell; it excites other cells to fire and in turn is reexcited by them. This regenerative excitatory feedback among the cells causes each of them to discharge repetitively at high frequency, and as the burst proceeds, the accumulating refractoriness of each cell increases. The burst is terminated when the excitatory input to each cell is no longer sufficient to overcome the increasing threshold for spike initiation. A silent period ensues until the same small cell, which recovers faster than the other cells, initiates a burst again. This mechanism is similar to one first proposed for lobster cardiac ganglia by Maynard (1955). A computer model has been described by Wilson (1966) and an electronic model by Lewis (1968).

The other mechanism assumes that one or more of the nine cells is capable of discharging spontaneously in bursts of spikes in isolation from the others. The burster neurons are coupled to each other by electrotonic or excitatory synaptic connections so that they start bursting within a few milliseconds of each other. Synaptic drive to even nonburster neurons assures that all nine burst together. This mechanism is similar to one proposed for lobster cardiac ganglia by Bullock and Terzuolo (1957), Otani and Bullock (1959 *a*, *b*) and Hartline (1967 *a*).

The relaxation oscillator used to describe the present results is in many ways consistent with either of the two classes of mechanisms, but on balance I am inclined towards the view presented by Hartline (1967 *a*) that bursts are generated by burst-generating neurons that are similar to pacemaker neurons of *Squilla* heart. If bursts are generated by means of mutual excitation among neurons, then the oscillator function could be a measure of refractoriness, accumulated from spike to spike during the burst period in an individual small cell and decaying exponentially during the silent period (Wilson, 1966; Mayeri, 1969). However, with this mechanism the responses of the system to brief shocks present a number of theoretical problems, the most serious of them being the interpretation of reset bursts. In this case the shock should produce a rapid decline in the value of the oscillator function, requiring either a rapid decline in the refractoriness of the neuron or a rapid facilitation of postsynaptic potentials. There is little experimental basis for expecting either of these phenomena (Hagiwara and Bullock, 1957). On the other hand, for bursts that are generated by burster neurons the most appropriate physical interpretation is that the first derivative of the oscillator function with respect to time (Fig. 3) is the membrane potential of an individual small cell, but without spike potentials or membrane capacitance. As with neurons known to be endogenous bursters (Alving, 1968; Frazier et al., 1967; Strumwasser, 1967), this "membrane potential" is bistable, being considerably more depolarized during the burst period than during the silent period. Its form is similar to the slow potentials recorded intracellularly from heart ganglion cells of the stomatopod, *Squilla* (Watanabe et al., 1967) or the crab, *Eriocheir japonicus* (Tazaki, 1971), which are probably burster neurons. In *Eriocheir* cells the slow potential remains after the spike potentials are abolished by addition of tetrodotoxin to the medium (Tazaki, 1971). During the burst period the slow potential of *Squilla* and *Eriocheir* neurons and the first derivative of the relaxation oscillator slowly decreases from a point of maximum depolarization at the start of the burst period, and, as one might expect from this, the frequency of spikes slowly declines during the burst period in each of these cardiac ganglia (Watanabe et al., 1967; Tazaki, 1971; Maynard, 1955; Hartline and Cooke, 1969). Also, during the silent period membrane potential slowly becomes more positive in each case. In *Squilla* cells, similar

to the present results, the plateau of depolarization during the burst is more easily abolished by stimulation near the end of the burst than near the beginning, and bursts that are terminated in this fashion are followed by shorter silent periods. Furthermore, a burst cannot be elicited by axonal stimulation early in the silent period, but can be elicited later in the silent period, and the elicited burst sets the rhythm of the bursts that follow (Watanabe et al., 1967). These considerations support the interpretation that in the lobster cardiac ganglion bursts are generated by endogenous burster neurons and that the excitatory synaptic connections among the cells (see Mayeri, 1973) have ancillary functions.

An equation which has the first derivative of the oscillatory function as its solution is $\ddot{v} + f(\dot{v})\dot{v} + v = 0$, where $v = \dot{H}$ and $f(\dot{v})\dot{v} = (\mathrm{d}/\mathrm{d}t)(F(\dot{v}))$. The general form of this equation may be appropriate for other oscillatory excitable membranes, especially ones where transmembrane potentials can be easily recorded. It should be possible to find $f(\dot{v})$ from a direct measure of the transmembrane potential over one complete cycle of oscillation by taking the first and second derivative of the membrane potential (without the spikes) at each point in the cycle and solving the differential equation for $f(\dot{v})$. Unfortunately, lobster cardiac ganglia are not presently amenable to this analysis because the small cells are difficult to penetrate with intracellular electrodes (Hagiwara, 1961).

The late Dr. Donald M. Wilson was a constant source of inspiration and assistance. I am also grateful to Dr. Edwin R. Lewis for valuable discussions, and to Drs. C. H. F. Rowell, B. Mulloney, and E. R. Kandel for comments on the manuscript.

Computer time was provided by the University of California (Berkeley) Computer Center.

This study was supported by a grant from the Public Health Service (GM 35007).

This study is based on part of a thesis submitted for the Ph.D. degree at the University of California, Berkeley, November, 1969.

Received for publication 9 November 1972.

REFERENCES

ALVING, B. O. 1968. Spontaneous activity in isolated somata of *Aplysia* pacemaker neurons. *J. Gen. Physiol.* **51**:29.

BULLOCK, T. H., and C. A. TERZUOLO. 1957. Diverse forms of activity in the somata of spontaneous and integrating ganglion cells. *J. Physiol.* **138**:341.

EVOY, W. H., and M. J. COHEN. 1972. Central and peripheral control of arthropod movements. *Adv. Comp. Physiol. Biochem.* **4**:225.

FRAZIER, W. T., E. R. KANDEL, I. KUPFERMANN, R. WAZIRI, and R. E. COGGESHALL. 1967. Morphological and functional properties of identified neurons in the abdominal ganglion of *Aplysia californica*. *J. Neurophysiol.* **30**:1288.

HAGIWARA, S. 1961. Nervous activities of the heart in Crustacea. *Ergeb. Biol.* **24**:287.

HAGIWARA, S., and T. H. BULLOCK. 1957. Intracellular potentials in pacemaker and integrative neurons of the lobster cardiac ganglion. *J. Cell. Comp. Physiol.* **50**:25.

HARTLINE, D. K. 1967 *a*. Integrative physiology of the lobster cardiac ganglion. Ph.D. Thesis, Harvard University, Cambridge.

HARTLINE, D. K. 1967 *b*. Impulse identification and axon mapping of the nine neurons in the cardiac ganglion of the lobster *Homarus americanus*. *J. Exp. Biol.* **47**:327.

HARTLINE, D. K., and I. M. COOKE. 1969. Postsynaptic membrane response predicted from presynaptic input pattern in lobster cardiac ganglion. *Science* (*Wash. D.C.*). **164**:1080.

LEWIS, E. R. 1968. Using electronic circuits to model simple neuroelectric interactions. *Proc. Inst. Electr. Electron. Eng.* **56**:931.

MAYERI, E. 1969. Integration in the lobster cardiac ganglion. Ph.D. Thesis, University of California, Berkeley.

MAYERI, E. 1973. Functional organization of the cardiac ganglion of the lobster, *Homarus americanus*. *J. Gen. Physiol.* **62**:448.

MAYNARD, D. M. 1955. Activity in a crustacean ganglion. II. Pattern and interaction in burst formation. *Biol. Bull.* (*Woods Hole*). **109**:420.

OTANI, T. and T. H. BULLOCK. 1959 *a*. Responses to depolarizing currents across the membrane of some invertebrate ganglion cells. *Anat. Rec.* **128**:599.

OTANI, T. and T. H. BULLOCK. 1959 *b*. Effects of presetting the membrane potential of the soma of spontaneous and integrating ganglion cells. *Physiol. Zool.* **32**:104.

STOKER, J. J. 1950. Non-Linear Vibrations in Electrical and Mechanical Systems. Interscience Pubs., Inc., John Wiley & Sons, Inc. New York.

STRUMWASSER, F. 1967. Types of information stored in single neurons. *In* Invertebrate Nervous Systems, C. A. G. Wiersma, editor. University of Chicago Press, Chicago. 291.

TAZAKI, K. 1971. The effects of tetrodotoxin on the slow potential and spikes in the cardiac ganglion of the crab, *Eriocheir japonicus*. *Jap. J. Physiol.* **21**:529.

WATANABE, A., S. OBARA, and T. AKIYAMA. 1967. Pacemaker potentials for the periodic burst discharge in the heart ganglion of a stomatopod, *Squilla oratoria*. *J. Gen. Physiol.* **50**:839.

WILSON, D. M. 1966. Central nervous mechanisms for the generation of rhythmic behaviour in arthropods. *Symp. Soc. Exp. Biol.* **20**:199.

WILSON, D. M. 1970. Neural operations in arthropod ganglia. *In* The Neurosciences: Second Study Program, F. O. Schmitt, editor. The Rockefeller University Press, New York. 397.